

Fauna associated with shallow-water methane seeps in the Laptev Sea

Andrey A Vedenin ^{Corresp., 1}, Sergey V Galkin ², Valentin N Kokarev ^{3, 4}, Margarita V Chikina ⁴, Alexander B Basin ⁴, Andrey V Gebruk ²

¹ Laboratory of plankton communities structure and dynamics, P.P. Shirshov Institute of Oceanology, Moscow, Russia

² Laboratory of Ocean Bottom Fauna, P.P. Shirshov Institute of Oceanology, Moscow, Russia

³ Faculty of Biosciences and Aquaculture, Nord University, Bodø, Norway

⁴ Laboratory of Ecology of Coastal Bottom Communities, P.P. Shirshov Institute of Oceanology, Moscow, Russia

Corresponding Author: Andrey A Vedenin
Email address: urasterias@gmail.com

Background. Methane seeps provide environment for unique benthic ecosystems in the deep-sea dependent on chemosynthetic organic matter. In contrast, in shallow waters there is little or no effect of methane seeps on macrofauna. In the present study we focused on the recently described methane discharge area at the northern Laptev Sea shelf. The aim of this work was to describe the shallow-water methane seep fauna and to understand whether the differences in community structure between the methane seep and background areas exist.

Methods. Samples of macrofauna were taken during three expeditions of RV *Akademik Mstislav Keldysh* in 2015, 2017 and 2018 using 0.1 m² grabs and the Sigsbee trawl. 21 grabs and two trawls in total were taken at two methane seep sites named *Oden* and *C15*, located at depths of 60-70 m. For control, three 0.1 m² grabs were taken in area without methane seepage.

Results. The abundance of macrofauna was higher at methane seep stations, compared to non-seep. Cluster analysis revealed five station groups corresponding to control area, *Oden* site and *C15* site (the latter represented by three groups). Taxa responsible for differences between the station groups were mostly widespread Arctic species, that were more abundant in samples from methane seep sites. However, large densities of symbiotrophic siboglinids *Oligobrachia* sp. were found exclusively at methane seep stations. In addition, several species presumably new to science were found at several methane seep stations, including the gastropod *Frigidalvania* sp. and the polychaete *Ophryotrocha* sp. The fauna at control stations was represented only by well-known and widespread Arctic taxa. Number of station groups revealed from *C15* stations and high species richness in *C15* trawl sample comparing to *Oden* indicated higher diversity of microniches within the *C15* site. The development of specific methane seep communities at such shallow depths can be related to pronounced oligotrophic environment on the northern Siberian shelf.

1 Fauna associated with shallow-water methane seeps in the Laptev Sea

2

3 Andrey A. Vedenin¹, Sergey V. Galkin¹, Valentin N. Kokarev^{1,2}, Margarita V. Chikina¹,
4 Alexander B. Basin¹, Andrey V. Gebruk¹

5

6 ¹ – P.P. Shirshov Institute of Oceanology, Moscow, Russia

7 ² – Nord University, Faculty of Biosciences and Aquaculture, Bodø, Norway

8

9 Corresponding Author:

10 Andrey A. Vedenin¹

11 Nahimovskiy Prospekt 36, Moscow, 117997, Moscow, Russia

12 Email address: urasterias@gmail.com

13

14 Abstract

15 **Background.** Methane seeps provide environment for unique benthic ecosystems in the deep-sea
16 dependent on chemosynthetic organic matter. In contrast, in shallow waters there is little or no
17 effect of methane seeps on macrofauna. In the present study we focused on the recently
18 described methane discharge area at the northern Laptev Sea shelf. The aim of this work was to
19 describe the shallow-water methane seep fauna and to understand whether the differences in
20 community structure between the methane seep and background areas exist.

21 **Methods.** Samples of macrofauna were taken during three expeditions of RV *Akademik Mstislav*
22 *Keldysh* in 2015, 2017 and 2018 using 0.1 m² grabs and the Sigsbee trawl. 21 grabs and two
23 trawls in total were taken at two methane seep sites named *Oden* and *C15*, located at depths of
24 60-70 m. For control, three 0.1 m² grabs were taken in area without methane seepage.

25 **Results.** The abundance of macrofauna was higher at methane seep stations, compared to non-
26 seep. Cluster analysis revealed five station groups corresponding to control area, *Oden* site and
27 *C15* site (the latter represented by three groups). Taxa responsible for differences between the
28 station groups were mostly widespread Arctic species, that were more abundant in samples from
29 methane seep sites. However, large densities of symbiotrophic siboglinids *Oligobrachia* sp. were
30 found exclusively at methane seep stations. In addition, several species presumably new to
31 science were found at several methane seep stations, including the gastropod *Frigidalvania* sp.
32 and the polychaete *Ophryotrocha* sp. The fauna at control stations was represented only by well-
33 known and widespread Arctic taxa. Number of station groups revealed from *C15* stations and
34 high species richness in *C15* trawl sample comparing to *Oden* indicated higher diversity of
35 microniches within the *C15* site. The development of specific methane seep communities at such
36 shallow depths can be related to pronounced oligotrophic environment on the northern Siberian
37 shelf.

38

39 **Introduction**

40 Methane gas seeping from the seafloor, similar to hydrothermal vents, can provide
41 environmental conditions for unique fauna largely independent of photosynthetic primary
42 production (Van Dover, 2000). Distinct faunal response at methane seeps (also known as “cold
43 seeps”) is associated with certain increase of total abundance/biomass and presence of unique
44 taxa absent in background areas. This pattern has been described from many areas of the Ocean
45 (Baker & German, 2004; Levin, 2005). These taxa either develop symbiotic relationships with
46 methanotrophic or sulphide-oxidizing bacteria or feed directly on benthic or suspended bacterial
47 matter. As a next trophic level, predators feeding exclusively on such taxa may be present
48 (Gebruk, 2002; Dando, 2010).

49 In the Arctic Ocean, several methane seep ecosystems have been discovered and
50 investigated. The most studied include the Håkon Mosby mud volcano in the Norwegian Sea
51 (Gebruk et al., 2003) and several sites around Svalbard and at Vestnesa Ridge (Åström et al.,
52 2016; Åström et al., 2018). Other described cold seeps include the Lofoten-Vesterålen
53 continental margin area (Sen et al., 2019a) and mud volcanoes in the Beaufort Sea (Paull et al.,
54 2015). The cold seeps inhabited by specific benthic macrofauna are mostly located below the
55 photic zone (depth >200 m both around Svalbard and at Håkon Mosby) (Gebruk et al., 2003;
56 Åström et al., 2016). At the same time, areas with extensive methane discharge located at
57 shallow depths (e.g. in the Norwegian and White Seas at depths <100 m) have no or minor
58 response of macrofauna (Savvichev et al., 2004; Levin, 2005). In general, a depth boundary is
59 observed between shallow-water cold seeps and their “deep-sea” counterparts at approximately
60 200 m (Tarasov et al., 2005; Dando, 2010). One of possible reasons for this boundary is the
61 origin of organic matter: at depths <200 m photosynthetic organic matter is more available for
62 benthic consumers due to stronger benthic-pelagic coupling. At greater depth, however, the
63 amount of photosynthetic organic matter decreases and chemosynthesis starts to play a
64 significant role for local organic matter production. Therefore, despite the presence of methane
65 and sulfides (unfavorable for most organisms), unique and diverse ecosystems can develop at
66 deep-sea cold seeps (summarized by Dando, 2010).

67 Fauna associated with cold seeps in the Arctic includes symbiotrophic siboglinid
68 polychaetes and thyasirid bivalves, but mainly consists of species not unique for methane seeps.
69 Widespread Arctic species tend to aggregate in habitats around methane seepage sites (Gebruk et
70 al., 2003; Åström et al., 2016; Åström, Oliver & Carroll, 2017). Arctic cold seep assemblages are
71 characterized by the dominance of frenulate siboglinid worms, while large chemosymbiotrophic
72 methane seep taxa (vestmentiferan worms, bathymodioline and vesicomid bivalves) are absent
73 (Sen et al. 2018). Common effect of methane seeps on benthic communities around the Ocean is
74 an increased abundance and biomass of regular allochthonous taxa compared to the background
75 (Gebruk, 2002; Levin, 2005). The diversity values at cold seeps are not higher than in the
76 background, though recent results obtained from the southwestern Barents Sea showed increased
77 taxonomic richness within the seepage sites (Sen et al., 2019b).

78 In the Siberian Arctic, areas of intense methane discharge (methane seeps) were discovered
79 on the outer shelf of the Laptev Sea in 2008 (Yusupov et al. 2010). Further research revealed
80 numerous gas flares in the northern Laptev Sea shelf (Lobkovsky et al., 2015; Shakhova 2015).
81 Within this area specific microbial communities based on methane oxidation were discovered
82 (Savvichev et al. 2018). Characteristic features and structural control of methane seep fields in
83 this area were given in Baranov et al. (2019). It is suggested that the methane seeping occurs
84 through the fault system belonging to Laptev Sea Rift system and Khatanga-Lomonosov Fracture
85 Zone located between the Eurasian and North American Tectonic Plates. The faults may conduit
86 the gas from reservoirs deep in the sediment below the caprock formed by permafrost and gas
87 hydrates (Baranov et al., 2019). Within the seeping area, multiple bacterial mats and occasional
88 methane bubbles and carbonate crusts were observed (Baranov et al., 2019).

89 Notably, the methane associated fauna was registered on the Laptev Sea shelf and slope
90 much earlier: during expeditions of RV *Polarstern* in 1993 and 1995 five species of siboglinids
91 were found in this area in the depth range 50-2000 m (Sirenko et al., 2004), which is more than
92 anywhere else in the high Arctic.

93 We examined benthic communities associated with methane seeps in the Laptev Sea at two
94 sites: *C15*, centred around 76°47.4'N and 125°49.5'E with depths 70-73 m and *Oden*, centred
95 around 76.894°N and 127.798°E, with depths 63-67 m. Preliminary description of benthic fauna
96 observed on video was published by Baranov et al. (2019). The aim of this study is to describe
97 further the biological peculiarities of the methane seep fauna and to reveal the differences in

98 either integral community characteristics or distribution of certain species between the methane
99 seep and background areas. We hypothesized that the seep sites are different from the non-seep
100 in terms of general community characteristics and certain species distribution.

101

102 **Materials & Methods**

103 Samples of macrofauna were taken during three expeditions of RV *Akademik Mstislav Keldysh*
104 in 2015 (AMK-63), 2017 (AMK-69) and 2018 (AMK-72) on the northern Laptev Sea shelf, in
105 the area of active methane discharge. The gears used for sampling were the *Okean* (in 2015) and
106 *Van Veen* (in 2017-2018) grabs (0.1 m² sampling area) and the *Sigsbee* trawl (2 m frame width)
107 (Eleftheriou & McIntyre, 2005). 21 grab and two trawl stations were performed in total at three
108 sites: on two methane seep fields (12 grabs and one trawl at *C15* and six grabs and one trawl at
109 *Oden*) and at the control site with no methane seeping (three grabs) (Fig. 1). A single trawl was
110 taken at each seep site to minimize the possible ecosystem damage from this gear. In 2015 three
111 seep stations were selected above the present gas flares visible on echo-sounder. Three more
112 grabs were taken ~200 m away from the nearest gas flare to catch background community. In
113 2017 and 2018 station selection was based largely on the previously mapped methane flares. All
114 the 2017 and 2018 grabs were taken above the gas flares (Fig. 1). Station data with coordinates
115 and depths are shown in Table 1. For additional information on methane seep fields see Flint et
116 al. (2018) and Baranov et al. (2019).

117

118 Table 1. Data on stations used in the present study. For trawl stations coordinates and depth of start and
119 end are given.

120

121 Fig. 1. Study area.

122 Enlarged maps show sampling sites and corresponding stations. Detailed bathymetry is only available for
123 *C15* and *Oden* sites; white circles indicate previously recorded gas flares (Baranov et al., 2019). Dotted
124 line at *Oden* site enclosed map shows the approximate perimeter of seeping area.

125

126 Sediment from grab samples was washed by hand through the 0.5 mm mesh size sieve, and
127 fixed with buffered 4% formalin solution afterwards. Two grab samples from the expedition in
128 2018 (Sts. 5947-3 at *C15* and 5953-2 at *Oden* site) were fixed with 96% ethanol. A 10-litre
129 subsample of sediment taken from each trawl catch was washed through the 1 mm mesh size
130 sieve and then fixed with neutralized 4% formalin. The material obtained was analyzed in the

131 laboratory; all macrofaunal organisms were identified to the lowest possible taxonomical level
132 with the help of taxonomical experts (see Acknowledgements) and counted. Species from grab
133 samples were weighed (wet weight, all specimens of each species at a time). Mollusks were
134 weighed with shells, polychaetes with calcareous (spirorbids) or mucous tubes (*Spiochaetopterus*
135 *typicus* and siboglinids) were weighed with tubes. Density and biomass were calculated per
136 square meter in case of grabs. Dominant species were distinguished by biomass. For trawl
137 samples we calculated the contribution (in %) of each species to abundance. Biomass was not
138 measured for trawl samples due to poor state of preservation. For ethanol fixed samples from Sts.
139 5947-3 and 5053-2, the biomass loss was corrected using taxa-specific coefficients after
140 Brotskaya & Zenkevich (1939).

141 For grab samples total abundance, biomass, species richness (species number), Pielou
142 evenness, Hurlbert rarefaction index and Shannon-Wiener diversity index ($H' \ln$) were calculated
143 to get integral community characteristics. Abundance and biomass data from grab samples were
144 square root transformed to increase the role of rare taxa. The similarity between grab samples
145 and species was estimated using the quantitative index of Bray-Curtis. Clusters were built based
146 on similarity matrices using the unconstrained tree routine (UNCTREE); results were verified by
147 SIMPROF to distinguish different station groups with significant differences in species
148 composition. The results from cluster analysis were verified by non-metric multidimensional
149 scaling (n-MDS). Clusters revealed by these methods were defined as separate station groups in
150 terms of quantitative taxonomical similarity. Shade plots were built to visualize the species
151 abundance and biomass differences between the stations and species in clusters. The Kruskal-
152 Wallis test was used to verify differences in certain taxa distribution between station groups.
153 Results were corrected using the Tukey's pairwise post-hoc test. Species-individuals
154 accumulation curves were plotted for each station group (McCune, Grace & Urban, 2002; Clarke
155 & Gorley, 2015).

156 For all species present in any station group, an algorithm estimating the likelihood of
157 accidental catch was applied. If a uniform distribution of species between two sampling efforts A
158 and B is assumed, the probability of species absence at each station of B-sampling would be $(1-$
159 $P_A)^{N(B)}$, where $N(B)$ is the number of stations in B-sampling and P_A is the species occurrence
160 (the proportion of stations where the species was present) in A-sampling. Using this equation, the
161 likelihood of accidental absence of any species in either station group can be estimated. The

162 number of grabs required for species catch in B-sampling can be calculated by the equation: $n =$
163 $\lg(\alpha) \lg(1-P_A)^{-1}$, where α is the likelihood of species finding in B-sampling taken as 0.99
164 (Azovsky, 2018; Vedenin et al., 2019).

165 For trawl samples, the species rank distributions were plotted. Species richness, Pielou
166 evenness, Hurlbert rarefaction index and Shannon-Wiener diversity index were calculated using
167 the taxa-percentage values. Differences between trawl catches were estimated by similarity
168 percentage routine (SIMPER).

169 Statistical analyses were performed in Primer V6, V7 and Past 3.0 software (Clarke &
170 Warwick, 2001; Hammer, 2013; Clarke & Gorley, 2015).

171

172 **Results**

173 A total of 289 taxa of benthic macrofauna were identified in grab and trawl samples. In grab
174 samples, density varied in the wide range from 580 ind. m^{-2} (St. 5624-3, Control site) to 9880
175 ind. m^{-2} (St. seep-3, C15 site). Biomass ranged from 16.28 g ww m^{-2} (St. seep-1, C15 site) to
176 405.79 g ww m^{-2} (St. 5623-3, Oden site). The list of all identified taxa from trawl and grab
177 samples, with values of abundance and biomass is given in the Supplementary 1.

178

179 Fig. 2. UNCTREE analysis with SIMPROF results (A) and non-metric multidimensional scaling plot (B)
180 of grab stations using the Bray-Curtis similarity index.

181 Square root transformed biomass data are used. Dashed lines connect statistically unreliable groupings (p
182 > 0.05). Green lines indicate SIMPROF groups.

183

184 **Grab samples**

185 Unconstrained tree with SIMPROF analysis revealed five significantly distinct groups of
186 samples at the similarity level of 50 (Fig. 2). The UNCTREE parameters are shown in
187 Supplementary 2. The groups partly corresponded with the station locations and
188 presence/absence of methane seeps (*Control*, *C15* and *Oden* sites). To avoid a mix-up between
189 the station groups and seeping sites hereinafter the corresponding names are used with either –
190 station group or –site ending.

191

192 Fig. 3. The species-individuals accumulation curves for the station groups.

193 Colors are the same as in Figure 2.

194

195 **Characteristics of station groups**

196 The *Control* station group included three stations located between methane seep sites (Fig. 1).
197 The bivalve *Portlandia arctica* was dominant by biomass at all three stations; the starfish
198 *Ctenodiscus crispatus* and the bivalve *Macoma calcarea* played a secondary role. Due to the low
199 number of samples, the species-individuals accumulation curve did not reach the saturation point
200 (Fig. 3). Compared to other groups, the values of density and species richness were the lowest at
201 Control, whereas the evenness was the highest (Fig. 4).

202 The *C15-seep a* station group included five stations, all within the *C15* seep site. In this
203 group, biomass and diversity values were relatively low. Dominant species in this group were the
204 bivalve *Nuculana pernula*, the siboglinid *Oligobrachia* sp. and the polychaete *Cistenides*
205 *hyperborea*. Species-individuals accumulation curve in this group reached saturation due to the
206 largest number of samples (Fig. 3).

207 The *C15-seep b* station group consisted of only two stations from *C15* site. This group
208 demonstrated the highest abundance values and the lowest biomass values owing to high
209 abundance of small polychaetes *Cossura longocirrata*, *Micronephthys minuta* and *Ophryotrocha*
210 sp. at some stations (Fig. 4, Supplementary 1).

211 The *Oden* station group included six stations, all located within the *Oden* seep site. Values
212 of biomass, species richness and diversity indices in this group were the highest among all
213 station groups (Fig. 4). The main dominant species were the siboglinid *Oligobrachia* sp. and the
214 polychaetes *Myriochele heeri* and *Nephtys ciliata*.

215
216 Fig. 4. Univariate characteristics of identified clusters.

217 Mean values of total density, biomass, species richness, Pielou evenness, Hurlbert rarefaction
218 index and Shannon-Wiener index with standard deviation are shown. Exact values of these
219 characteristics are shown in Supplementary 3.

220

221 The last group *C15 background* contained five stations taken within the *C15* site. Three of
222 these stations (Sts. background-1, 2 and 3) were taken several hundred meters away from active
223 methane seeps. Two stations (5947-1 and 5947-3) were planned as active seep stations.
224 Accidentally, they were taken in the seep background area according to taxa composition and
225 following analysis. Taxonomical composition at these stations was similar to that in the *Control*
226 group, with the bivalve *Portlandia arctica* being the dominant species. Bivalves *Yoldiella*

227 *lenticula* and *Y. solidula* were subdominant. In this station group, the biomass values were the
228 lowest, other general community characteristics were intermediate (Fig. 4). As with the *Control*
229 group, *C15 background* did not reach the saturation point at species-individuals accumulation
230 plot (Fig. 3).

231

232 ***Comparison of seep and non-seep station groups***

233 General community characteristics in the station groups appeared different in abundance,
234 biomass and diversity (Fig. 4, Supplementary 3). The abundance of several taxa was significantly
235 different in four station groups (Fig. 5). The Kruskal-Wallis test showed that differences in
236 abundance of at least ten species are statistically reliable (Table 2). The seep sites were
237 characterized by higher density of the polychaetes *Tharyx* sp. and *Cistenides hyperborea*, the
238 bivalve *Macoma calcarea* and the ophiuroid *Ophiocten sericeum*. On the contrary, the bivalve
239 *Portlandia arctica* was markedly more abundant in *Control* and, to a lesser extent, in *C15*
240 *background* station groups (Fig. 5). Notable were extreme densities of small polychaetes at some
241 seep stations, including *Cossura longocirrata* and *Ophtyotrocha* sp. (Fig. 5A) at *C15 seep b*.

242

243 Fig. 5. Shade plot of species square root transformed abundance (A) and biomass (B) at stations arranged
244 by clusters.

245 The species list is reduced to 20 most important taxa. Order of stations and colors the same as in Figure 2.

246 Taxa grouped in clusters using UPGMA algorithm based on index of association.

247

248 Certain species present at some methane seep sites were completely absent at the non-seep
249 sites (Fig. 5). Among them, at least four species (the polychaete *Spiochaetopterus typicus*, the
250 siboglinid *Oligobrachia* sp., the bivalve *Axinopsida orbiculata* and the amphipod *Pleusymtes*
251 *pulchellus*) were present only at *C15* and *Oden* sites not randomly. At least one species, the
252 undescribed gastropod *Frigidalvania* sp., was present only in *Oden* station group and absent
253 elsewhere not randomly (Table 3). The estimated number of grabs required to catch the latter
254 species was slightly lower than the number of grabs taken.

255

256 Table 2. Results of the Kruskal-Wallis and Tukey's post-hoc tests for taxa with different abundance
257 values in five station groups. Mean abundance in each station group is shown. Taxa are arranged
258 according to *p*-value. Pairs in post-hoc column indicate significant comparisons (Tukey's *p* < 0.05).

259 1 – *Control* group; 2 – *C15 background* group; 3 – *Oden* group; 4 – *C15-seep a* group; 5 – *C15-seep-b*
260 group.

261
262
263
264
265
266

Table 3. Likelihood of not finding a species calculated for species present only at methane seep sites and only at the *Oden* site.

267 ***Trawl samples***

268 The overall Bray-Curtis similarity between the two trawls was 65.6%. Species ranking graphs
269 showed high level of dominance by abundance for both trawl stations (Fig. 6). The dominant
270 species in both trawls was the ophiuroid *Ophiocten sericeum*: 37% of the total abundance at *C15*
271 and 46% at *Oden*. The second most abundant species at *C15* was the gastropod *Frigidalvania* sp.
272 (12%) and at *Oden* the bivalve *Yoldiella solidula* (11%). Ten most abundant species accounted
273 for >70% of the total abundance in both trawls (Fig. 6).

274
275 Fig. 6. Species ranking for *C15* and *Oden* trawl samples.
276 The most numerous species are indicated. X-axis is logarithmic.
277

278 Species richness, Pielou evenness, Hurlbert rarefaction for 100 individuals and Shannon-
279 Wiener index are shown in Table 4. Diversity was higher in the *Oden*-trawl than in the *C15*-
280 trawl, similar to results based on grab samples. However, the species richness (as well as the
281 total amount of individuals) in the *C15*-trawl was higher than in the *Oden*-trawl (Table 4,
282 Supplementary 1).

283 Species responsible for taxonomical difference between the two trawl samples are shown
284 in Table 5. Most notable is a high amount of the gastropod *Frigidalvania* sp. at *C15*. At *Oden*
285 *Frigidalvania* sp. was also present, but in much smaller densities (only 2.3 % of the total
286 abundance). In addition, *C15*-sample differs from *Oden* by high amount of various filter-feeders
287 including 6 species of sponges (with *Craniella polyura* being most numerous), at least 6 species
288 of cnidarians, 17 species of bryozoans and 3 species of tunicates (Supplementary 1).

289 At *C15* trawl sample, a large piece of carbonate crust was found. Cavities of its pores were
290 inhabited by numerous polychaetes, typical also for the soft sediments around the seepage area
291 (e.g. members of families Nephthyidae, Nereididae, Oweniidae and Terebellidae, see
292 Supplementary 1), and by several filter-feeders (Hydrozoa).

293

294 Table 4. Species richness, Pielou evenness, Hurlbert rarefaction for 100 individuals and Shannon-Wiener
295 index calculated for trawl samples.

296

297 Table 5. Similarity percentage routine for trawl samples.

298 Species with contribution >0.5% are shown. Species more abundant at *C15* are marked with bold.

299

300 ***Comparison of C15 and Oden sites***

301 All gears showed significant differences between the *C15* and *Oden* sites expressed in different
302 taxonomical composition and quantitative characteristics. The Bray-Curtis similarity between the
303 sites according to the grab samples and trawl samples was 26.2 and 65.6, respectively. The main
304 differences in species composition included the high abundance of the sponge *Craniella polyura*
305 and the gastropod *Frigidalvania* sp. at *C15* site and higher numbers of the ophiuroid *Ophiocten*
306 *sericeum* at *Oden* site.

307 The grab data indicated a high level of heterogeneity of benthic fauna on the scale of
308 several meters at both seep-sites. Some species formed patches, for example *Oligobrachia* sp.,
309 *Cossura longocirrata* and *Ophryotrocha* sp., being extremely numerous at several grab stations.
310 There were also species with rather uniform distribution based on combined data, for example
311 *Ophiocten sericeum*. According to the cluster analysis, the *C15* site is more heterogenic forming
312 at least three different species complexes within its area (Fig. 2). Dissimilarity within the *C15*
313 and *Oden* sites was 64.7 and 26, respectively (Supplementary 2).

314 Dominant species were different in grab and trawl samples. The dominant species in trawls
315 at both methane seep sites was the ophiuroid *Ophiocten sericeum*. Whereas based on grab data,
316 the dominants at seep sites were the siboglinid *Oligobrachia* sp., the bivalve *Nuculana pernula*
317 and the polychaete *Myriochele heeri*.

318

319 **Discussion**

320 ***Integral community parameters: methane seep vs. non-seep***

321 The abundance of macrofauna was higher at the seep stations compared to the background. In
322 addition, at *Oden* site the biomass was higher compared to non-seep sites. Increased values of

323 abundance and biomass have been reported from both hydrothermal vents and cold seeps all over
324 the world. In the Arctic, a twofold increase of biomass compared to control sites was observed at
325 cold seeps south off Svalbard (mean values of 20.7 vs. 9.8 g ww m⁻²), the abundance increase
326 was less prominent (770 vs. 590 ind. m⁻²) (Åström, 2016). For the Håkon Mosby mud volcano,
327 the comparison of abundance and biomass with the background is not available. In our study, the
328 abundance at the methane seep sites *C15* and *Oden* was more than four times higher than at the
329 control. However, differences in biomass although pronounced were not statistically reliable.
330 Increased biomass in seep habitats is commonly explained by enhanced organic matter content
331 and habitat heterogeneity (Gebruk et al. 2003; Sen et al. 2018).

332 Pielou's evenness was distinctly higher at the *Control* and *C15 background* station
333 groups, which reflects the increased dominance of certain species at seep stations compared to
334 non-seep. Many authors reported high abundance and biomass values of one to few dominant
335 species at various cold seeps (Gebruk et al. 2003; Åström, 2016; Åström et al., 2018). This can
336 be caused by conditions less favorable for some background species, but more favorable for
337 symbiotrophs or grazers (summarized in Dando, 2010).

338 The cold seeps usually demonstrate lower diversity values compared to the background
339 areas (Levin, 2005). However, combined species list from grab and trawl samples showed a big
340 diversity taking into account that only two trawls were sampled. Our studies at Siberian shelf
341 using the same gear under same conditions obtained less than 150 species per trawl (Galkin &
342 Vedenin, 2015; Vedenin, Galkin & Kozlovsky, 2015), while a total of 203 species were found in
343 a single *C15* sample. The unusually large diversity may reflect a higher amount of microniches
344 within the *C15* site. This is indirectly confirmed by lower similarity values observed between all
345 *C15* grab samples. Higher habitat heterogeneity at seep sites can increase the overall diversity of
346 benthic fauna (Gebruk et al. 2003; Levin, 2005). The scale of heterogeneity is hard to assess, but
347 based on stations coordinates and the fact that stations 5947-1 and 5947-2 from *C15*-site were
348 grouped in *C15 background*, while station 5947-2 was grouped as *C15-seep a* we can assume
349 that the scale is less than five meters (distance between these stations) (Fig. 1; Table 1).

350 In addition, the diversity values at *Oden* station group were significantly higher than at
351 other sites. The reasons for this are unknown so far, since no environmental parameters measured
352 directly at benthic stations are available. Interestingly, the peculiarly higher values of diversity

353 within the cold seeps are known only for the seep areas in the Arctic, e.g. for the Vestnesa Ridge
354 (Åström et al., 2018) and for the South-Western Barents Sea (Sen et al., 2019b).

355

356 ***Common shelf taxa responsible for differences in station groups***

357 The station groups revealed by UNKTREE and n-MDS analysis largely corresponded to the
358 geographical position of the *C15*, *Oden* and control sites. A number of common species widely
359 distributed across the Siberian shelf (see Supplementary 1, Sirenko, 2001) were largely
360 responsible for increased integral community parameters in our study. Most of these taxa are
361 listed in Table 2. Among such species (based on grab samples) were the polychaetes
362 *Spiochaetopterus typicus*, *Cossura longocirrata* and *Tharyx* sp., the bivalve *Macoma calcarea*,
363 the amphipod *Pleusymtes pulchella* and the ophiuroid *Ophiocten sericeum*. In addition, based on
364 trawl data, the sponge *Craniella polyura* was present in high densities at the *C15* site, together
365 with other filter-feeders including cnidarians and bryozoans. Apparently the same species
366 aggregations were visible on the video reported by Baranov et al. (2019). All these species were
367 previously reported from a wide range of areas of the Laptev Sea and adjacent regions (Sirenko
368 et al., 2004).

369 The increased density of common taxa at deep-sea hydrothermal vents and cold seeps is a
370 well-known phenomenon usually explained by increased availability of organic matter in these
371 habitats (Hessler & Kaharl, 1995; Levin, 2005). In the Arctic, the increased biomass and
372 abundance of common allochthonous species was reported for the Håkon Mosby mud volcano
373 (Rybakova et al., 2013), Svalbard (Åström et al., 2016) and Vestnesa Ridge cold seeps (Åström
374 et al., 2018). Also, a significant increase of abundance of filter feeders (especially sponges) was
375 shown for the Aurora Seamount on the Gakkel Ridge, the only investigated hydrothermal vent in
376 the Central Arctic Ocean (Boetius, 2015).

377

378 Fig. 7. Taxa found only at seep stations.

379 A – *Oligobrachia* sp. (left – tube with several fragments enlarged; center – complete specimen extracted
380 from tube; right – anterior and posterior fragments of the specimen); B – *Frigidalvania* sp.; C –
381 *Ophryotrocha* sp. (upper left – several specimens, total view; upper right – anterior fragment; lower –
382 enlarged parapodia); D – *Axinopsida orbiculata*. Photos by A. Vedenin and V. Kokarev.

383

384 *Taxa specific for methane seep sites*

385 The main species marking the methane seeps in our study was the siboglinid *Oligobrachia* sp.
386 (Fig. 7a). This species was present at every seep station and absent at every background/control
387 station. This species is morphologically very close to *Oligobrachia haakonmosbiensis* originally
388 described from the Håkon Mosby mud volcano from the depth of ~1200 m (Smirnov, 2000).
389 Colonies of *O. haakonmosbiensis* with the biomass reaching 350 g ww m⁻² were reported from
390 this area (Gebruk et al., 2003). Recent phylogenetical analyses showed that the species from the
391 Laptev Sea belongs to a separate, undescribed species of *Oligobrachia* (Sen et al., 2018). In the
392 Laptev Sea, *Oligobrachia* sp. is known from different localities, seep and noon-seep, occurring
393 in a wide depth range 100-2166 m (Buzhinskaja, 2010). Our record at 63 m is the shallowest for
394 this species, with high population density and biomass: >1000 ind. m⁻² and 45 g ww m⁻² at Sts.
395 2623-1 and 5953-2 (*Oden* site). Several specimens from 2015-samples (erroneously identified as
396 *O. haakonmosbiensis*) were investigated using transmission electron microscopy (Savvichev et
397 al., 2018). Interestingly, metanotrophic bacteria were found inside its trophosome. Usually the
398 endosymbionts of Siboglinids are represented by sulphide-oxidizing bacteria (Rodrigues et al.,
399 2011; Lee et al., 2019).

400 Some samples from the seep sites besides the siboglinids also were marked by several
401 species of mollusks. The gastropod *Frigidalvania* sp. (Rissoidea) occurred in high density at *CI5*
402 site: up to 2340 ind. m⁻² and 25 g ww m⁻² at St. 5625-3 (Fig. 7b). According to trawl samples,
403 this species occurs at *Oden* site, but in a few numbers. This species is new to science. Large
404 numbers of unknown rissoid gastropods were previously reported from the Håkon Mosby,
405 referred to as *Alvania* sp. in Gebruk et al. (2003). Later, the stable isotope analysis has shown
406 that the rissoids at Håkon Mosby are grazing on bacterial mats (Decker & Olu, 2012). Another
407 rissoid gastropod, *Pseudosetia griegi*, was observed grazing on bacterial mats at the hot vent
408 Loki Castle on the Mohn's Ridge (Sweetman et al., 2013). At the recently investigated Lofoten
409 canyon seep site dense aggregations of unidentified rissoids were observed from ROV (Sen et
410 al., 2019a). Based on the details available from the published photo, we suggest that the
411 gastropods are very likely to belong to genus *Frigidalvania*, based on the shell shape and rusty-
412 brownish periostracum (Sen et al., 2019a, see Fig. 4b). Unfortunately, in our study we were not
413 able to identify the behavior or lifestyle of *Frigidalvania* sp. This species remained unnoticed in
414 the video data due to its small size (Baranov et al., 2019). However, multiple bacterial mats

415 observed from video-transects and caught by box corer provide an opportunity for such species
416 to graze on them (Savvichev et al., 2018; Baranov et al., 2019). Other species common at seep
417 sites and lacking in the background was the thyasirid bivalve *Axinopsida orbiculata* (Fig. 7d).
418 Some species of thyasirids are known as symbiotrophic, however, the information on symbiotic
419 bacteria in the gills of *A. orbiculata* is controversial: Zhukova, Kharlamenko & Gebruk (1991)
420 have demonstrated the presence of bacteria in bivalve specimens from the Kraternaya Bight, the
421 Kuril Islands, whereas according to Dufour (2005) this species lacks bacterial symbionts. It is
422 possible that *A. orbiculata* is attracted by increased food availability at seep sites, same as
423 another bivalve, *Macoma calcarea*, which is also common in seep background areas (Fig. 5).
424 Overall, no bivalves restricted to cold seeps are known so far in the Arctic with the exception of
425 two large thyasirids recently described by few empty shells (Åström, Oliver & Carroll, 2017) and
426 Pleistocene subfossils (e.g. *Archivesica* spp., Sirenko et al., 2004; Hansen et al., 2017). The
427 subfossils suggest that previously the Arctic cold seeps (and possibly hydrothermal vents) were
428 inhabited by richer fauna that became extinct after Quaternary glaciation.

429 Notable is the high density (>3600 ind. m⁻²) of the dorvilleid polychaete *Ophryotrocha* sp.
430 in one grab sample at *C15-seep b* station group (Supplementary 1 (Fig. 7c). At least 15 species of
431 *Ophryotrocha* have been described from reducing habitats (Taboada et al., 2013; Salvo et al.,
432 2014; Ravara et al., 2015), including two species considered as obligate for cold seeps in the
433 Kagoshima Bay, Japan (Miura, 1997). On the other hand, many species of this genus are
434 common in regular marine ecosystems including Arctic seas (Sirenko, 2001).

435 Another taxon common in reducing habitats is tanaid crustaceans (Tanaidacea). In our
436 material three species were present (Supplementary 1), all widely distributed in the Arctic
437 (Sirenko, 2001). The density of tanaids in our samples was low, although this taxon was reported
438 in high densities from the Håkon Mosby (Gebruk et al., 2003) and the Vestnesa Ridge (Åström et
439 al., 2018) with several species (described as new) restricted to the methane seep habitats
440 (Błazewicz-Paszkowycz and Bamber, 2011). It seems likely that many species of tanaids remain
441 unidentified and diversity in this taxon remains underestimated owing to difficulties of
442 identification of these small crustaceans (summarized by Błazewicz-Paszkowycz & Bamber,
443 2011). The low number of tanaids in our samples could be a result of a too large sieve mesh size
444 used onboard (see Materials & Methods). Tanaids commonly are < 0.5 mm in size and require a
445 corresponding mesh size to be found (Pavithran et al., 2009).

446 Overall, considering grab and trawl data combined, all the seep-specific taxa were the same
447 at both seep sites. The only exception is the polychaete *Ophryotrocha* sp., which could be missed
448 from the *Oden* trawl sample due to the large sieve mesh size (Supplementary 1).

449

450 ***Presence of specific benthic communities at C15 and Oden***

451 Up to now no distinct macrofaunal changes in response to methane seeps were reported from the
452 Arctic Ocean at depths < 80 m. In general, at depths <200 m both hydrothermal vents and cold-
453 seeps are usually colonized by a subset of the local fauna (Tarasov et al., 2005; Dando, 2010).
454 Some species notable at shallow-water methane seeps belong to opportunistic taxa common in
455 various reducing habitats. These include siboglinid polychaetes and thyasirid bivalves reported
456 from Skagerrak, Kattegat, coastal areas of Florida, Japan, New Zealand, New Guinea etc.
457 (Southward & Culter, 1986; Schmaljohann & Flügel, 1987; Schmaljohann et al., 1990;
458 Malakhov, Obzhairov & Tarasov, 1992; Gebruk, 2002). The isotope data suggest that food
459 sources of macrofauna at shallow-water methane seeps are largely photosynthesis-based (Levin,
460 2005). It was suggested that the faunistic depth boundary between the deep-sea and shallow-
461 water vents and seeps at approximately 200 m is controlled by the amount of organic matter
462 input from the photosynthetic production (decreasing below the photic zone) and the greater
463 number of predators at shallow depths. Definite seep-obligate species were not reported from
464 depths <200 m (Tarasov et al., 2005; Dando, 2010).

465 At the same time, methane seep habitats even at shallow depths increase a number of
466 microniches owing to increased organic matter availability, variety of substrates and repeated
467 disturbance (Dando, 2010). Shallow cold-seeps may therefore support greater species diversity
468 compared to the background. In our study at both methane seep sites, *C15* and *Oden*, integral
469 community characteristics were significantly different from those in non-seep areas, among other
470 things owing to presence of species obligate for reducing habitats. In addition, the communities
471 found at *C15* site formed several station groups and were more scattered at the n-MDS plot (Fig.
472 2A, B) which could indicate a larger diversity of microniches within this site. Large amount of
473 filter-feeders (Hydrozoa and Bryozoa) found in *C15*-trawl indicates the presence of hard
474 substrata (including carbonate crusts). The larger amount of microniches is partly supported by

475 the video-data, where the landscape within the active seepages was more complex than in non-
476 seep areas (Flint et al., 2018; Baranov et al., 2019).

477 Unfortunately, no environmental data except for the echo-sounding showing certain gas
478 flares and CTD-measurements obtained from the area of the seeps from two points away from
479 the benthic samples are available (Flint et al., 2018; Baranov et al., 2019). Nevertheless, we
480 suggest that response of macrofauna to methane seeps at shallow depths 60-70 m can be related
481 to very low primary productivity on the outer shelf of the Laptev Sea, dropping from ~720mg C
482 m⁻² per day at Lena river delta to <100 mg C m⁻² per day at 600 km (Sorokin & Sorokin, 1996)
483 during September. Outside short Arctic summer months, these values tend to zero. In these
484 extremely oligotrophic conditions, methane as a source of energy for the methane-oxidizing
485 bacteria stimulates the development of local patchy benthic communities even at a shallow
486 depth. As a comparison, the specific communities with siboglinids around Svalbard located at
487 similar latitude are developed only at depths >200 m (Åström et al., 2016). Unlike the Laptev
488 Sea shelf, the primary production south and west off Svalbard reaches much higher values up to
489 1800 mg C m⁻² per day during May blooms (Wassman et al., 2006). Furthermore, the Barents
490 Sea remains uncovered with ice during most of the year, while the Laptev Sea shelf is ice-free
491 during one to two months annually.

492 **Conclusions**

493 Our study is the first description of shallow-water methane seep communities in the Siberian
494 Arctic. On the northern Laptev Sea shelf, significant differences were found between two
495 methane seep sites (*C15* and *Oden*, located at depths of 63-73 m) and the background areas. The
496 differences included integral community parameters and presence at seep sites of species typical
497 for reducing habitats, such as siboglinids *Oligobrachia* sp. and thyasirid bivalves. Several
498 species at methane seeps are presumably new to science, including the gastropod *Frigidalvania*
499 sp. and the polychaete *Ophryotrocha* sp., found in large quantities at *C15* site. We suggest that
500 response of macrofauna to methane seeps at shallow depths is related to very low primary
501 productivity on the outer shelf of the Laptev Sea.

502

503 **Acknowledgements**

504 The authors would like to thank the Captain, crew members and shipboard parties of the RV
505 *Akademik Mstislav Keldysh* for multiple help with the work onboard during the 63, 69 and 72
506 expeditions. Our special thanks to Dr. Michael Flint for organizing the expeditions and for
507 informative discussions. We also thank Dr. Alexey Udalov and Dr. Elena Krylova for help in
508 identifying mollusks and crustaceans. This work was partly funded by RFBR Grants 18-04-
509 00206, 18-05-60053, 18-05-60228 and the State assignment of IORAS (theme No 0149-2019-
510 0009).

511 **References**

512

- 513 1. Åström, E. K., Carroll, M. L., Ambrose Jr, W. G., & Carroll, J. (2016). Arctic cold seeps in
514 marine methane hydrate environments: impacts on shelf macrobenthic community structure
515 offshore Svalbard. *Marine Ecology Progress Series*, 552, 1-18.
- 516 2. Åström, E. K., Oliver, P. G., & Carroll, M. L. (2017). A new genus and two new species of
517 Thyasiridae associated with methane seeps off Svalbard, Arctic Ocean. *Marine Biology*
518 *Research*, 13(4), 402-416.
- 519 3. Åström, E. K., Carroll, M. L., Ambrose Jr, W. G., Sen, A., Silyakova, A., & Carroll, J.
520 (2018). Methane cold seeps as biological oases in the high-Arctic deep sea. *Limnology and*
521 *Oceanography*, 63(S1), S209-S231.
- 522 4. Azovsky, A.I. (2018) Analysis of long-term biological data series: methodological problems
523 and possible solutions. *J Gene Biol (Moscow)* 79:329–341 [in Russian]
- 524 5. Baker, E. T., & German, C. R. (2004). On the global distribution of hydrothermal vent fields.
525 *Mid-Ocean Ridges: Hydrothermal Interactions Between the Lithosphere and Oceans*,
526 *Geophys. Monogr. Ser.*, 148, 245-266.
- 527 6. Baranov B., Galkin S., Vedenin A., Dozorova K., Gebruk A., Flint M. 2019. Methane seeps
528 on the outer shelf of the Laptev Sea: characteristic features, benthic fauna and structural
529 control. *Geophysical Research Letters*. [in press]
- 530 7. Błażewicz-Paszkwycz, M., & Bamber, R. N. (2011). Tanaidomorph Tanaidacea (Crustacea:
531 Peracarida) from mud-volcano and seep sites on the Norwegian Margin. *Zootaxa*, 3061, 1-35.
- 532 8. Boetius, A. (2015). The expedition PS86 of the Research Vessel POLARSTERN to the Arctic
533 Ocean in 2014. *Berichte zur Polar-und Meeresforschung = Reports on polar and marine*
534 *research*, 685, 1-132.
- 535 9. Brotskaya, V., Zenkevich, L., 1939. Quantitative account of the Barents Sea benthic fauna.
536 *Trudy VNIRO*, 4, 55-120. [in Russian]
- 537 10. Buzhinskaja, G. N. (2010). Illustrated keys to free-living invertebrates of Eurasian Arctic seas
538 and adjacent deep waters. Nemertea, Cephalorincha, Oligochaeta, Hirudinea, Pogonophora,
539 Echiura, Sipuncula, Phoronida and Brachiopoda, 2. 186 p.
- 540 11. Clarke, K.R., Warwick, R.M., 2001. *Changes in Marine Communities: An Approach to*
541 *Statistical Analysis and Interpretation* (2nd ed.). PRIMER-E, Plymouth
- 542 12. Clarke, K. R., Gorley, R. N. (2015). *Getting started with PRIMER v7. PRIMER-E: Plymouth,*
543 *Plymouth Marine Laboratory.*
- 544 13. Dando, P.R., 2010. Biological communities at marine shallow-water vent and seep sites. In:
545 Kiel S. (Ed.) *The Vent and Seep Biota*, Springer, Dordrecht, pp. 333-378.
- 546 14. Van Dover, C. (2000). *The ecology of deep-sea hydrothermal vents*. Princeton University
547 Press.
- 548 15. Decker C., & Olu K. (2012). Habitat heterogeneity influences cold-seep macrofaunal
549 communities within and among seeps along the Norwegian margin – Part 2: contribution of
550 chemosynthesis and nutritional patterns. *Marine Ecology*, 33(2), 231-245.
- 551 16. Dufour, S. C. (2005). Gill anatomy and the evolution of symbiosis in the bivalve family
552 Thyasiridae. *The Biological Bulletin*, 208(3), 200-212.
- 553 17. Eleftheriou A., McIntyre A. (2005). *Methods for the study of Marine benthos*. 3rd edn.
554 Blackwell Science, Oxford, UK. 418 p.

- 555 18. Flint M., Arashkevich E., Artemyev V., Baranov B., Bezzubova E., Belevich T., ... &
556 Shchuka S.A. Ecosystems of seas of Siberian Arctic. Materials of expeditionary research of
557 2015 and 2017. P.P. Shirshov Institute of oceanology, RAS. Moscow: 2018. 232 p. [in
558 Russian]
- 559 19. Galkin, S. V., & Vedenin, A. A. (2015). Macrobenthos of Yenisei Bay and the adjacent Kara
560 Sea shelf. *Oceanology*, 55(4), 606-613.
- 561 20. Gebruk A.V. Biology of hydrothermal vents. Moscow, KMK-Press, 2002. 543 p. [in Russian]
- 562 21. Gebruk, A. V., Krylova, E. M., Lein, A. Y., Vinogradov, G. M., Anderson, E., Pimenov, N.
563 V., ... & Crane, K. (2003). Methane seep community of the Håkon Mosby mud volcano (the
564 Norwegian Sea): composition and trophic aspects. *Sarsia*, 88(6), 394-403.
- 565 22. Hammer, Ø. 2013. PAST. Paleontological Statistics. Version 3.10. Reference manual. Natural
566 History Museum. University of Oslo.
- 567 23. Hansen, J., Hoff, U., Szytybor, K., & Rasmussen, T. L. (2017). Taxonomy and palaeoecology
568 of two Late Pleistocene species of vesicomid bivalves from cold methane seeps at Svalbard
569 (79° N). *Journal of Molluscan Studies*, 83(3), 270-279.
- 570 24. Hessler, R.R., Kaharl, V.A., 1995. The deep-sea hydrothermal vent community: an overview.
571 Seafloor hydrothermal systems. In: Humphris, S.E., Zierenberg, R.A., Mullineaux, L.S.,
572 Thomson, R.E. (Eds.), *Geophysical Monograph*, vol. 91. American Geo-physical Union, pp.
573 72-84.
- 574 25. Lee, D. H., Kim, J. H., Lee, Y. M., Jin, Y. K., Paull, C., Kim, D., & Shin, K. H. (2019).
575 Chemosynthetic bacterial signatures in Frenulata tubeworm *Oligobrachia* sp. in an active mud
576 volcano of the Canadian Beaufort Sea. *Marine Ecology Progress Series*, 628, 95-104.
- 577 26. Levin, L. A. (2005). Ecology of cold seep sediments: interactions of fauna with flow,
578 chemistry and microbes. In *Oceanography and Marine Biology* (pp. 11-56). CRC Press.
- 579 27. Lobkovsky, L. I., Nikiforov, S. L., Ananiev, R. A., Khortov, A. V., Semiletov, I. P.,
580 Jakobsson, M., & Dmitrievskiy, N. N. (2015). Recent geological-geomorphological processes
581 on the east Arctic shelf: Results of the expedition of the icebreaker Oden in 2014.
582 *Oceanology*, 55(6), 926-929.
- 583 28. Malakhov, V. V., Obzhairov, A. I., & Tarasov, V. G. (1992). Pogonophoran genus *Siboglinum*
584 in relation to zones of high concentrations of methane. *Doklady Akademii Nauk*, 135, 195-
585 197. [in Russian]
- 586 29. McCune, B., Grace, J.B., Urban, D.L., 2002. Analysis of Ecological Communities. Vol. Mj
587 Software Design., Gleneden Beach, Oregon, p. 28.
- 588 30. Miura, T. (1997). Two new species of the genus *Ophryotrocha* (Polychaeta, Iphitimiidae)
589 from Kagoshima Bay. *Bulletin of Marine Science*, 60(2), 300-305.
- 590 31. Paull, C. K., Dallimore, S. R., Caress, D. W., Gwiazda, R., Melling, H., Riedel, M., ... &
591 Sherman, A. (2015). Active mud volcanoes on the continental slope of the Canadian B
592 eaufort S ea. *Geochemistry, Geophysics, Geosystems*, 16(9), 3160-3181.
- 593 32. Pavithran, S., Ingole, B., Nanajkar, M., & Goltekar, R. (2009). Importance of sieve size in
594 deep-sea macrobenthic studies. *Marine Biology Research*, 5(4), 391-398.
- 595 33. Ravara, A., Marçal, A. R., Wiklund, H., & Hilário, A. (2015). First account on the diversity of
596 *Ophryotrocha* (Annelida, Dorvilleidae) from a mammal-fall in the deep-Atlantic Ocean with
597 the description of three new species. *Systematics and biodiversity*, 13(6), 555-570.
- 598 34. Rodrigues, C. F., Hilário, A., Cunha, M. R., Weightman, A. J., & Webster, G. (2011).
599 Microbial diversity in Frenulata (*Siboglinidae*, Polychaeta) species from mud volcanoes in the
600 Gulf of Cadiz (NE Atlantic). *Antonie Van Leeuwenhoek*, 100(1), 83-98.

- 601 35. Rybakova, E., Galkin, S., Bergmann, M., Soltwedel, T., & Gebruk, A. (2013). Density and
602 distribution of megafauna at the Håkon Mosby mud volcano (the Barents Sea) based on image
603 analysis. *Biogeosciences*, 10, 3359-3374.
- 604 36. Salvo, F., Wiklund, H., Dufour, S. C., Hamoutene, D., Pohle, G., & Worsaae, K. (2014). A
605 new annelid species from whalebones in Greenland and aquaculture sites in Newfoundland:
606 *Ophryotrocha cyclops*, sp. nov. (Eunicida: Dorvilleidae). *Zootaxa*, 3887(5), 555-568.
- 607 37. Savvichev A.S., Rusanov I.I., Yusupov S.K., Pimenov N.V., Lein A.Y., & Ivanov M.V. 2004.
608 The biogeochemical cycle of methane in the coastal zone and littoral of the Kandalaksha Bay
609 of the White Sea. *Microbiology*, 73(4), 457-468.
- 610 38. Savvichev, A. S., Kadnikov, V. V., Kravchishina, M. D., Galkin, S. V., Novigatskii, A. N.,
611 Sigalevich, P. A., ... & Flint, M. V. (2018). Methane as an organic matter source and the
612 trophic basis of a Laptev Sea cold seep microbial community. *Geomicrobiology journal*,
613 35(5), 411-423.
- 614 39. Schmaljohann, R., & Flügel, H. J. (1987). Methane-oxidizing bacteria in Pogonophora.
615 *Sarsia*, 72(1), 91-98.
- 616 40. Schmaljohann, R., Faber, E., Whitticar, M. J., & Dando, P. R. (1990). Co-existence of
617 methane-and sulphur-based endosymbioses between bacteria and invertebrates at a site in the
618 Skagerrak. *Marine Ecology Progress Series*, 61, 119-124.
- 619 41. Sen A., Duperron S., Hourdez S., Piquet B., Le'ger N., Gebruk A., Le Port A.S., Svenning
620 M.M., & Andersen A.C. (2018) Cryptic frenulates are the dominant chemosymbiotrophic
621 fauna at Arctic and high latitude Atlantic cold seeps. *PLoS ONE*, 13(12): e0209273.
- 622 42. Sen A., Himmler T., Hong W.L., Chitkara C., Lee R.W., Ferré B., ... & Knies J. (2019a).
623 Atypical biological features of a new cold seep site on the Lofoten-Vesterålen continental
624 margin (northern Norway). *Scientific reports*, 9(1), 1762.
- 625 43. Sen, A., Chitkara, C., Hong, W. L., Lepland, A., Cochrane, S., di Primio, R., & Brunstad, H.
626 (2019b). Image based quantitative comparisons indicate heightened megabenthos diversity
627 and abundance at a site of weak hydrocarbon seepage in the southwestern Barents Sea. *PeerJ*,
628 7, e7398.
- 629 44. Shakhova, N., Semiletov, I., Sergienko, V., Lobkovsky, L., Yusupov, V., Salyuk, A., ... &
630 Nicolsky, D. (2015). The East Siberian Arctic Shelf: towards further assessment of
631 permafrost-related methane fluxes and role of sea ice. *Philosophical Transactions of the Royal
632 Society A: Mathematical, Physical and Engineering Sciences*, 373(2052), 20140451.
- 633 45. Sirenko, B. I. (2001). List of species of free-living invertebrates of Eurasian Arctic seas and
634 adjacent deep waters. *Explorations of the fauna of the seas*, 51(59), 5-131.
- 635 46. Sirenko B., Denisenko S., Deubel H., & Rachor E. (2004). Deep water communities of the
636 Laptev Sea and adjacent parts of the Arctic Ocean. *Fauna and the ecosystems of the Laptev
637 Sea and adjacent deep waters of the Arctic Ocean. Explorations of the fauna of sea*, 54(62),
638 28-73.
- 639 47. Smirnov, R. V. (2000). Two new species of Pogonophora from the arctic mud volcano off
640 northwestern Norway. *Sarsia*, 85(2), 141-150.
- 641 48. Sorokin, Y. I., & Sorokin, P. Y. (1996). Plankton and primary production in the Lena River
642 estuary and in the south-eastern Laptev Sea. *Estuarine, Coastal and Shelf Science*, 43(4), 399-
643 418.
- 644 49. Southward, E. C., & Culter, J. K. (1986). Discovery of Pogonophora in warm shallow waters
645 of the Florida Shelf. *Marine Ecology Progress Series*, 28, 287-89.

- 646 50. Sweetman, A. K., Levin, L., Rapp, H. T., & Schander, C., 2013. Faunal trophic structure at
647 hydrothermal vents on the southern Mohn's Ridge, Arctic Ocean. *Marine Ecology Progress*
648 *Series*, 473, 115-131.
- 649 51. Taboada, S., Wiklund, H., Glover, A. G., Dahlgren, T. G., Cristobo, J., & Avila, C. (2013).
650 Two new Antarctic *Ophryotrocha* (Annelida: Dorvilleidae) described from shallow-water
651 whale bones. *Polar Biology*, 36(7), 1031-1045.
- 652 52. Tarasov, V. G., Gebruk, A. V., Mironov, A. N., & Moskalev, L. I. (2005). Deep-sea and
653 shallow-water hydrothermal vent communities: two different phenomena? *Chemical Geology*,
654 224(1-3), 5-39.
- 655 53. Vedenin, A. A., Galkin, S. V., & Kozlovskiy, V. V. (2015). Macrobenthos of the Ob Bay and
656 adjacent Kara Sea shelf. *Polar Biology*, 38(6), 829-844.
- 657 54. Vedenin, A., Mokievsky, V., Soltwedel, T., & Budaeva, N. (2019). The temporal variability
658 of the macrofauna at the deep-sea observatory HAUSGARTEN (Fram Strait, Arctic Ocean).
659 *Polar Biology*, p. 1-14. doi.org/10.1007/s00300-018-02442-8.
- 660 55. Wassmann, P., Reigstad, M., Haug, T., Rudels, B., Carroll, M. L., Hop, H., ... & Slagstad, D.
661 (2006). Food webs and carbon flux in the Barents Sea. *Progress in Oceanography*, 71(2-4),
662 232-287.
- 663 56. Yusupov, V. I., Salyuk, A. N., Karnaukh, V. N., Semiletov, I. P., & Shakhova, N. E. (2010).
664 Detection of methane ebullition in shelf waters of the Laptev Sea in the Eastern Arctic
665 Region. In: *Doklady Earth Sciences* (Vol. 430, No. 2, pp. 261-264). MAIK
666 Nauka/Interperiodica.
- 667 57. Zhukova, N.V., V.I. Kharlamenko & Gebruk A.V., 1991. Fatty acids of *Axinopsida*
668 *orbiculata* - potential for detection of symbiosis with chemoautotrophic bacteria. In, *Shallow*
669 *Water Vents and Ecosystem of J Kraternaya Bight (Volcano Ushishir. Kurile Islands)*, Vol. 1,
670 *Functional Characteristics, Part 11, Vladivostok, in press. [In Russian].*
671

Table 1 (on next page)

Data on stations used in the present study

For trawl stations coordinates and depth of start and end are given.

1 Table 1. Data on stations used in the present study. For trawl stations coordinates and depth of start and
 2 end are given.

Expedition, year	Station	Site	Gear	Latitude	Longitude	Depth (m)
AMK-63, 2015	seep-1	C15	Okean-0.1	76°46.376' N	125°49.641' E	72.0
	seep-2	C15	Okean-0.1	76°46.376' N	125°49.664' E	72.3
	seep-3	C15	Okean-0.1	76°46.379' N	125°49.618' E	72.4
	background-1	C15	Okean-0.1	76°46.375' N	125°50.346' E	73.0
	background-2	C15	Okean-0.1	76°46.366' N	125°50.366' E	73.0
	background-3	C15	Okean-0.1	76°46.365' N	125°50.339' E	73.0
	C15 trawl	C15	Sigsbee	76°46.483' N 76°46.447' N	125°50.843' E 125°48.231' E	71.5 72.0
AMK-69, 2017	5623-1	Oden	Van Veen-0.1	76°53.624' N	127°48.110' E	63.0
	5623-2	Oden	Van Veen-0.1	76°53.608' N	127°48.114' E	63.1
	5623-3	Oden	Van Veen-0.1	76°53.632' N	127°48.219' E	63.0
	Oden trawl	Oden	Sigsbee	76°53,667' N 76°53,566' N	127°48,157' E 127°49,075' E	63.0 63.0
	5624-1	Control	Van Veen-0.1	76°49.998' N	126°39.936' E	69.6
	5624-2	Control	Van Veen-0.1	76°50.003' N	126°39.896' E	69.7
	5624-3	Control	Van Veen-0.1	76°49.883' N	126°40.000' E	69.6
	5625-1	C15	Van Veen-0.1	76°46.438' N	125°49.417' E	70.8
	5625-2	C15	Van Veen-0.1	76°46.435' N	125°49.442' E	70.7
	5625-3	C15	Van Veen-0.1	76°46.413' N	125°49.437' E	70.6
AMK-72, 2018	5947-1	C15	Van Veen-0.1	76°46.847' N	125°49.085' E	72.3
	5947-2	C15	Van Veen-0.1	76°46.847' N	125°49.085' E	72.0
	5947-3	C15	Van Veen-0.1	76°46.848' N	125°49.097' E	72.0
	5953-1	Oden	Van Veen-0.1	76°53.554' N	127°48.405' E	63.0
	5953-2	Oden	Van Veen-0.1	76°53.551' N	127°48.409' E	63.0
	5953-3	Oden	Van Veen-0.1	76°53.567' N	127°48.400' E	63.0

3

4

Table 2 (on next page)

Results of the Kruskal-Wallis and Tukey's post-hoc tests for taxa with different abundance values in five station groups.

Mean abundance in each station group is shown. Taxa are arranged according to p -value. Pairs in post-hoc column indicate significant comparisons (Tukey's $p < 0.05$).

1 - *Control* group; 2 - *C15 background* group; 3 - *Oden* group; 4 - *C15-seep a* group; 5 - *C15-seep-b* group.

1 Table 2. Results of the Kruskal-Wallis and Tukey's post-hoc tests for taxa with different abundance
 2 values in five station groups. Mean abundance in each station group is shown. Taxa are arranged
 3 according to *p*-value. Pairs in post-hoc column indicate significant comparisons (Tukey's $p < 0.05$).

Species	Mean abundance in station groups					Kruskal-Wallis		Post-hoc
	1	2	3	4	5	<i>H</i> (chi ²)	<i>p</i>	
<i>Oligobrachia</i> sp.	0	0	63.0	14.6	53.5	15.86	0.00211	no values
<i>Yoldiella lenticula</i>	0.7	12.6	1.0	8.8	2.0	15.32	0.00362	2-1; 2-3; 2-5
<i>Cistenides hyperborea</i>	0	0.4	0.2	4.4	5.5	13.14	0.00378	no values
<i>Tharyx</i> sp.	2.3	6.0	32.5	3.8	2.5	14.70	0.00511	3-1; 3-2; 3-4; 3-5
<i>Spiochaetopterus typicus</i>	0	0	3.0	0.6	0	9.85	0.01151	no values
<i>Yoldiella solidula</i>	9.3	44.0	23.5	19.6	5.0	12.51	0.01391	no values
<i>Cossura longocirrata</i>	0	0	0.2	0.6	199.0	6.40	0.02177	no values
<i>Ophiecten sericeum</i>	0.3	3.8	6.3	4.8	26.5	10.38	0.03252	4-1; 4-2; 4-3; 4-5
<i>Portlandia arctica</i>	0	14.6	0	0.8	0.5	7.40	0.03257	no values
<i>Pleusymtes pulchella</i>	0	0	0.5	1.2	3.5	7.273	0.03463	no values
<i>Frigidalvania</i> sp.	0	0	0	59.8	29.5	5.15	0.05565	no values
<i>Anobothrus gracilis</i>	0	0	1.2	0.2	0	5.06	0.05839	no values
<i>Axinopsida orbiculata</i>	0	1.6	9.2	2.8	14.5	6.36	0.12860	no values
<i>Paroediceros lynceus</i>	0	0	0	0.8	4.0	2.57	0.13980	no values
<i>Haploops tubicola</i>	0.3	1.4	0.2	0	0	3.83	0.14310	no values

4 1 – Control group; 2 – C15 background group; 3 – Oden group; 4 – C15-seep a group; 5 – C15-seep-b
 5 group.
 6

Table 3 (on next page)

Likelihood of not finding a species calculated for species present only at methane seep sites and only at the *Oden* site.

¹ - Species absent not accidentally.

1 Table 3. Likelihood of not finding a species calculated for species present only at methane seep sites and
 2 only at the *Oden* site.

Species	Species occurrence	Likelihood of not finding	Number of grabs	
			Required for finding ($\alpha = 0.99$)	Taken
<i>Species present at C15-seep a, C15-seep b and Oden and absent at C15 background and Control sites</i>				
<i>Spiochaetopterus typicus</i> ¹	0.62	0.000	4.8	8
<i>Cossura longocirrata</i>	0.38	0.021	9.5	8
<i>Anobothrus gracilis</i>	0.38	0.021	9.5	8
<i>Oligobrachia sp.</i> ¹	1.00	0.000	1.0	8
<i>Axinopsida orbiculata</i> ¹	0.77	0.000	3.1	8
<i>Paroedicerus lynceus</i>	0.23	0.123	17.6	8
<i>Pleusymtes pulchella</i> ¹	0.53	0.002	6.0	8
<i>Species present at Oden and absent at C15-seep a and C15-seep b</i>				
<i>Frigidalvania sp.</i> ¹	0.57	0.006	5.4	6
<i>Portlandia arctica</i>	0.43	0.035	8.2	6
<i>Paroedicerus lynceus</i>	0.43	0.035	8.2	6

3 ¹ - Species absent not accidentally

4

Table 4(on next page)

Species richness, Pielou evenness, Hurlbert rarefaction for 100 individuals and Shannon-Wiener index calculated for trawl samples.

1 Table 4. Species richness, Pielou evenness, Hurlbert rarefaction for 100 individuals and Shannon-Wiener
2 index calculated for trawl samples.

Trawl	Species richness	Pielou evenness	ES (100)	Shannon-Wiener index
<i>C15</i>	203	0.55	29.97	2.92
<i>Oden</i>	167	0.56	33.02	2.86

3

Table 5 (on next page)

Similarity percentage routine for trawl samples. Species with contribution >0.5% are shown.

Species more abundant at *C15* are marked with bold.

1 Table 5. Similarity percentage routine for trawl samples. Species with contribution >0.5% are shown.

Species	Abundance (%)		Average dissimilarity	Contribution, %	Cumulative, %
	<i>C15</i>	<i>Oden</i>			
<i>Frigidalvania</i> sp.	12.05	2.37	4.84	14.06	14.06
<i>Ophiocten sericeum</i>	37.32	45.55	4.11	11.94	26.00
<i>Yoldiella lenticula</i>	7.37	1.11	3.13	9.08	35.08
<i>Yoldiella solidula</i>	7.82	10.89	1.54	4.46	39.55
<i>Portlandia arctica</i>	2.56	0.15	1.21	3.51	43.05
<i>Laona finmarchica</i>	1.60	0.00	0.80	2.32	45.38
<i>Phascalion strombus</i>	1.95	0.36	0.80	2.31	47.69
<i>Myriochele heeri</i>	0.42	1.82	0.70	2.03	49.72
<i>Micronephthys minuta</i>	0.16	1.47	0.65	1.90	51.62
<i>Craniella polyura</i>	1.30	0.00	0.65	1.88	53.50
<i>Pholoe longa</i>	1.38	2.62	0.62	1.79	55.29
<i>Munnopsis typica</i>	0.67	1.84	0.59	1.70	56.99
<i>Scoletoma fragilis</i>	0.28	1.17	0.45	1.30	58.30
<i>Paraediceros lynceus</i>	1.80	0.92	0.44	1.28	59.58
<i>Rostroculodes hanseni</i>	0.00	0.88	0.44	1.28	60.85
<i>Nothria hyperborea</i>	0.10	0.90	0.40	1.16	62.01
<i>Solariella obscura</i>	0.90	0.13	0.39	1.13	63.14
<i>Tharyx</i> sp.	0.04	0.67	0.31	0.91	64.05
<i>Axinopsida orbiculata</i>	0.00	0.61	0.30	0.88	64.93
<i>Brada villosa</i>	0.66	0.06	0.30	0.86	65.79
<i>Arrhis phyllonyx</i>	0.25	0.82	0.28	0.83	66.62
<i>Terebellides</i> aff. <i>stroemii</i>	0.86	1.42	0.28	0.82	67.44
<i>Similipecten</i>	0.68	0.15	0.27	0.78	68.22
<i>Cylichna occulta</i>	0.74	0.21	0.27	0.77	68.99
<i>Yoldiella frigida</i>	0.15	0.63	0.24	0.70	69.69
<i>Cossura longocirrata</i>	0.04	0.52	0.24	0.70	70.39
<i>Sabinea septemcarinata</i>	0.09	0.57	0.24	0.69	71.08
<i>Nymphon hirtipes</i>	0.10	0.57	0.23	0.67	71.76
<i>Cuspidaria glacialis</i>	0.80	0.38	0.21	0.61	72.37
<i>Brada incrustata</i>	0.04	0.46	0.21	0.61	72.98
<i>Lepidepecreum umbo</i>	0.42	0.02	0.20	0.58	73.56
<i>Ephesiella abyssorum</i>	0.01	0.40	0.19	0.56	74.12
<i>Nuculana pernula</i>	0.54	0.92	0.19	0.56	74.67
<i>Rozinante fragilis</i>	0.51	0.15	0.18	0.53	75.20
<i>Philine lima</i>	0.00	0.36	0.18	0.52	75.72
<i>Pleusymtes pulchellus</i>	0.36	0.71	0.17	0.51	76.22
<i>Owenia polaris</i>	0.07	0.42	0.17	0.50	76.72

2 Species more abundant at *C15* are marked with bold

Figure 1

Study area.

Enlarged maps show sampling sites and corresponding stations. Detailed bathymetry is only available for *C15* and *Oden* sites; white circles indicate previously recorded gas flares (Baranov et al., 2019). Dotted line at *Oden* site enclosed map shows the approximate perimeter of seeping area.

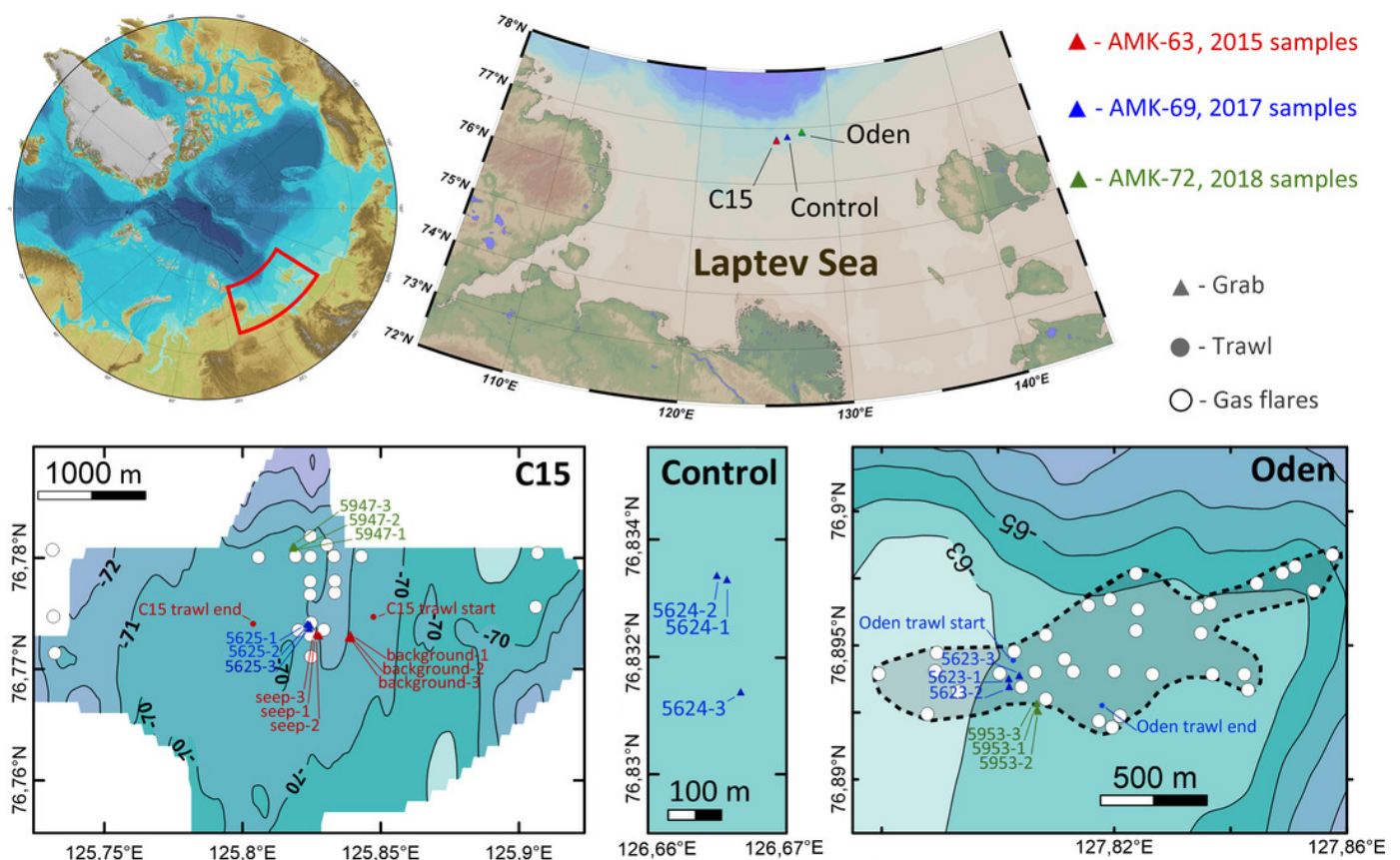
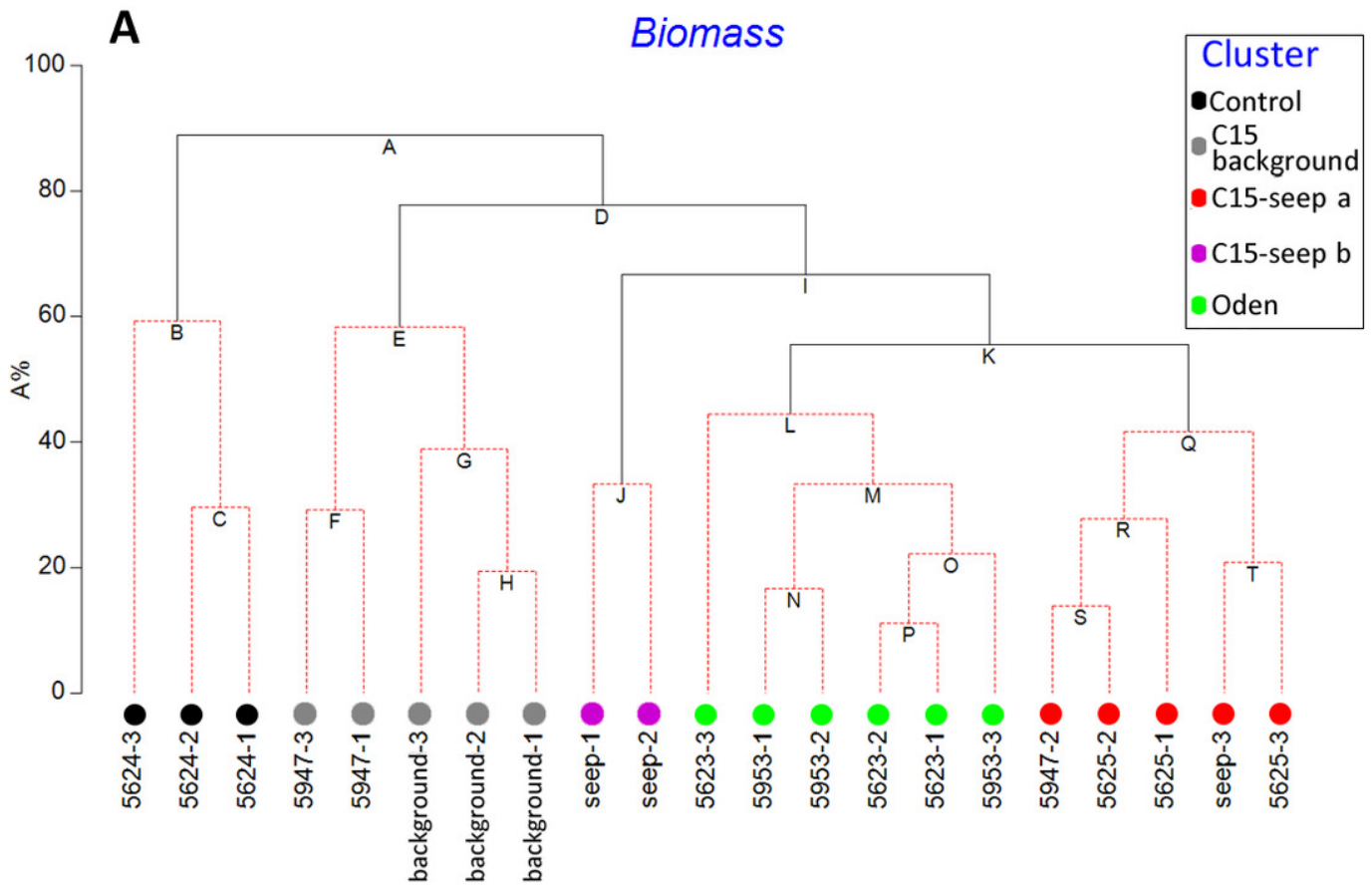


Figure 2

UNCTREE analysis with SIMPROF results (A) and non-metric multidimensional scaling plot (B) of grab stations using the Bray-Curtis similarity index.

Square root transformed biomass data are used. Dashed lines connect statistically unreliable groupings ($p > 0.05$). Green lines indicate SIMPROF groups.



B *Biomass*
Non-metric MDS

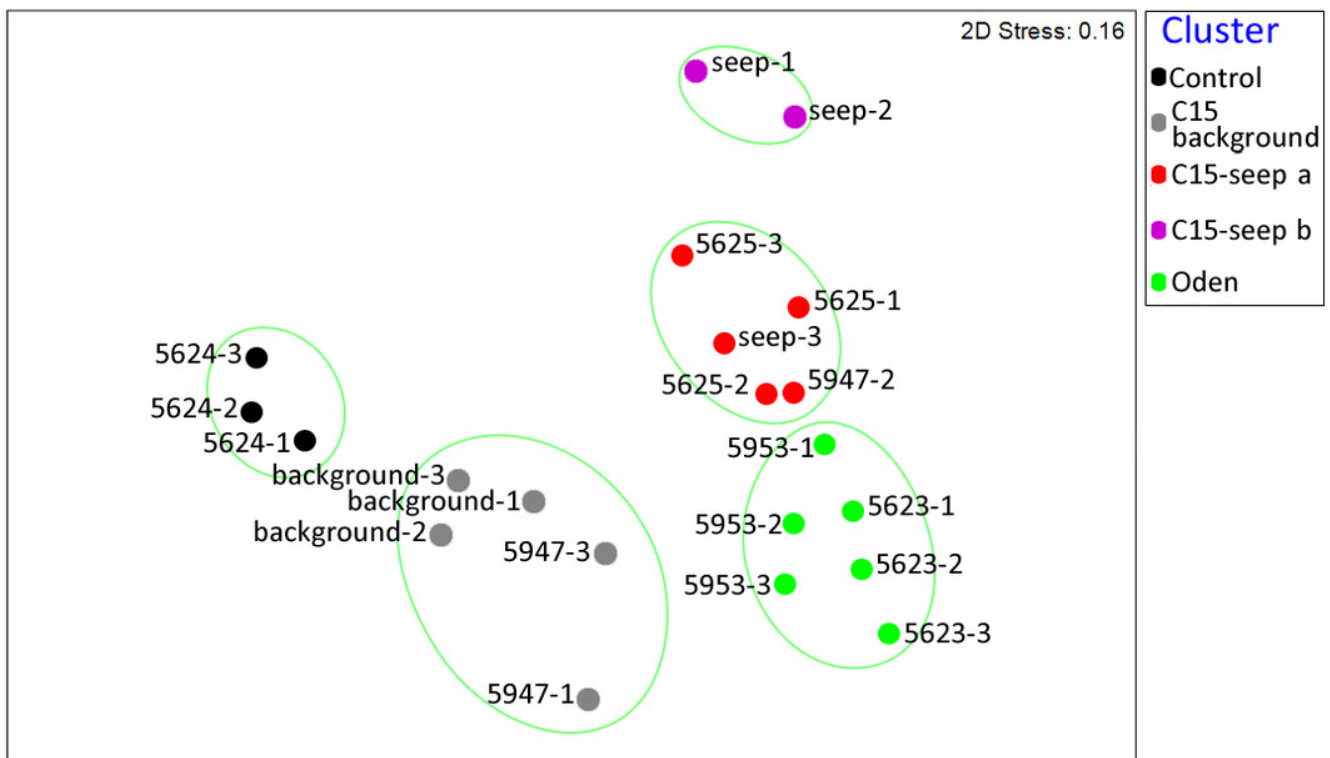


Figure 3

The species-individuals accumulation curves for the station groups.

Colors are the same as in Figure 2.

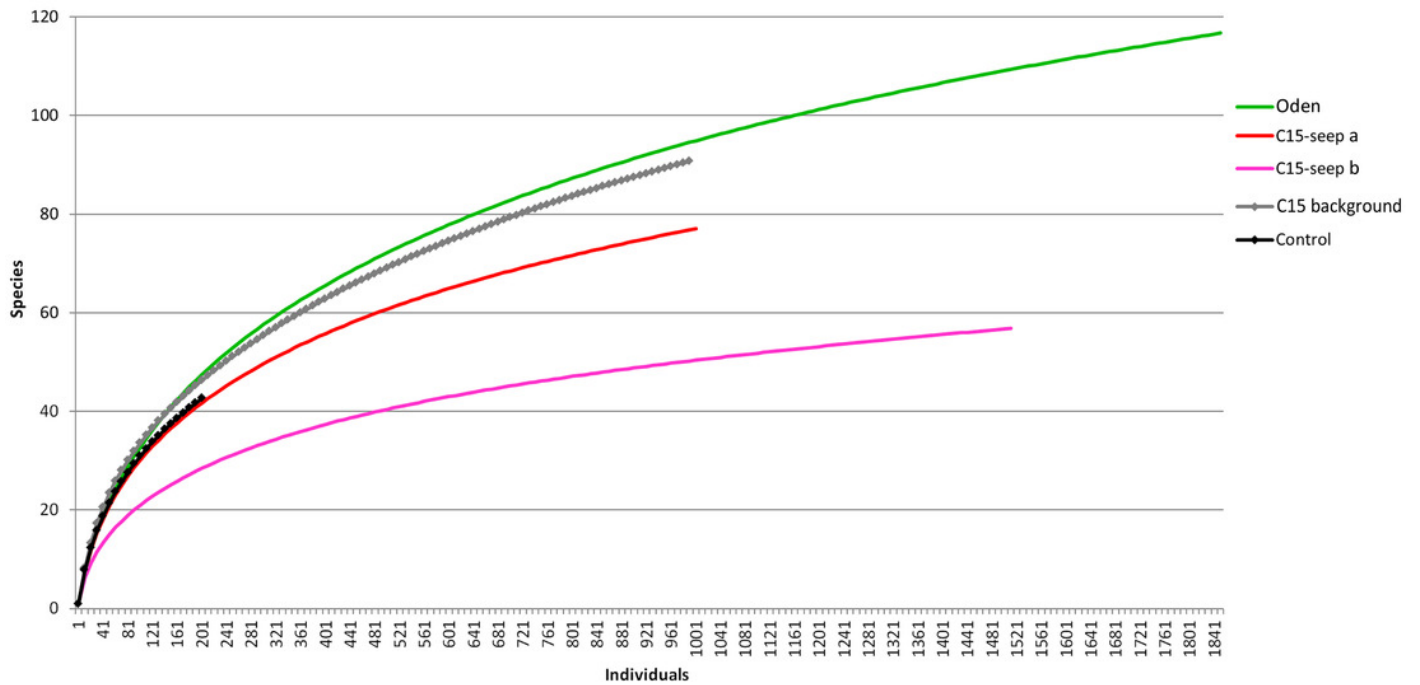


Figure 4

Univariate characteristics of identified clusters.

Mean values of total density, biomass, species richness, Pielou evenness, Hurlbert rarefaction index and Shannon-Wiener index with standard deviation are shown. Exact values of these characteristics are shown in Supplementary 3.

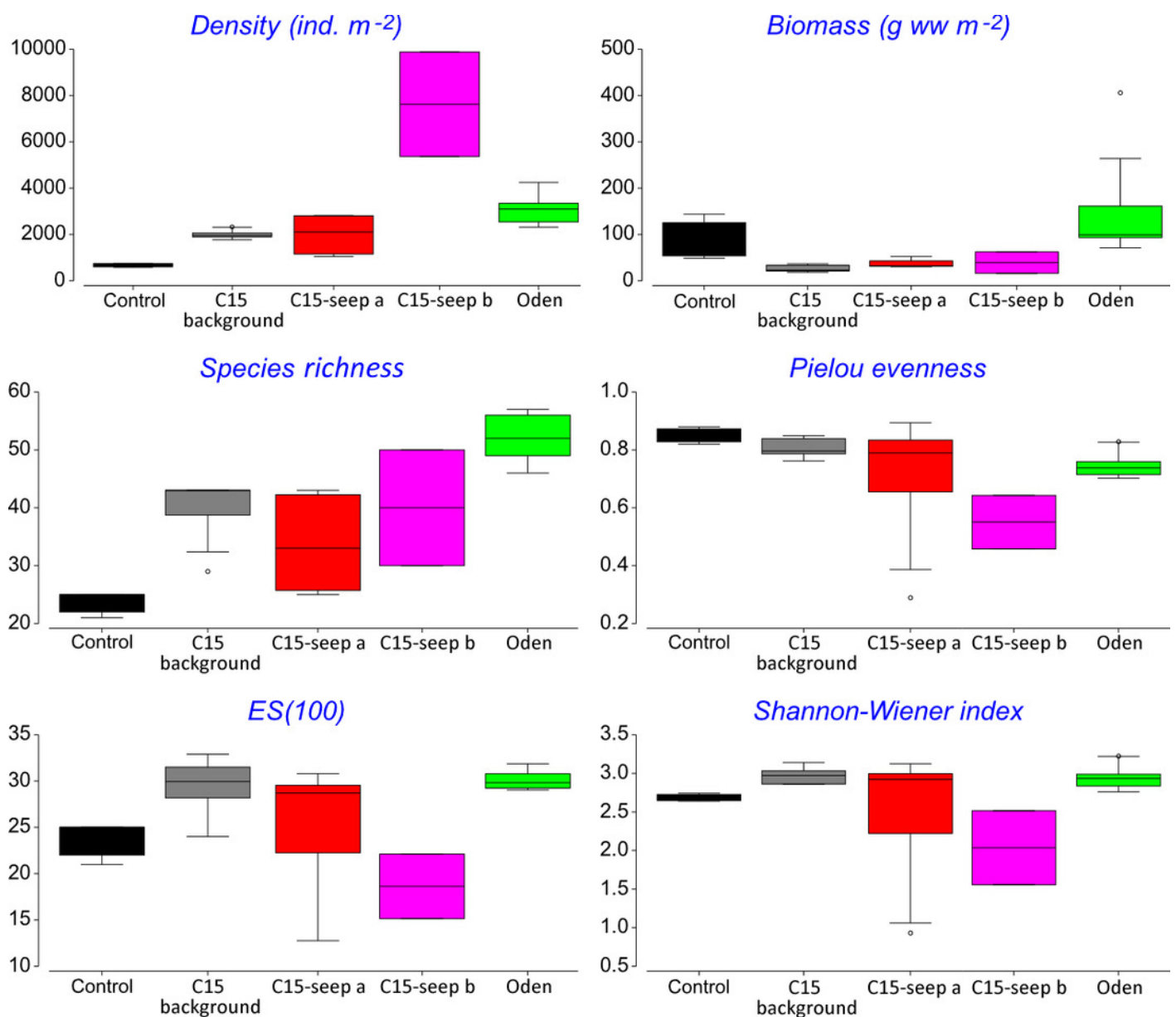


Figure 5

Shade plot of species square root transformed abundance (A) and biomass (B) at stations arranged by clusters.

The species list is reduced to 20 most important taxa. Order of stations and colors the same as in Figure 2. Taxa grouped in clusters using UPGMA algorithm based on index of association.

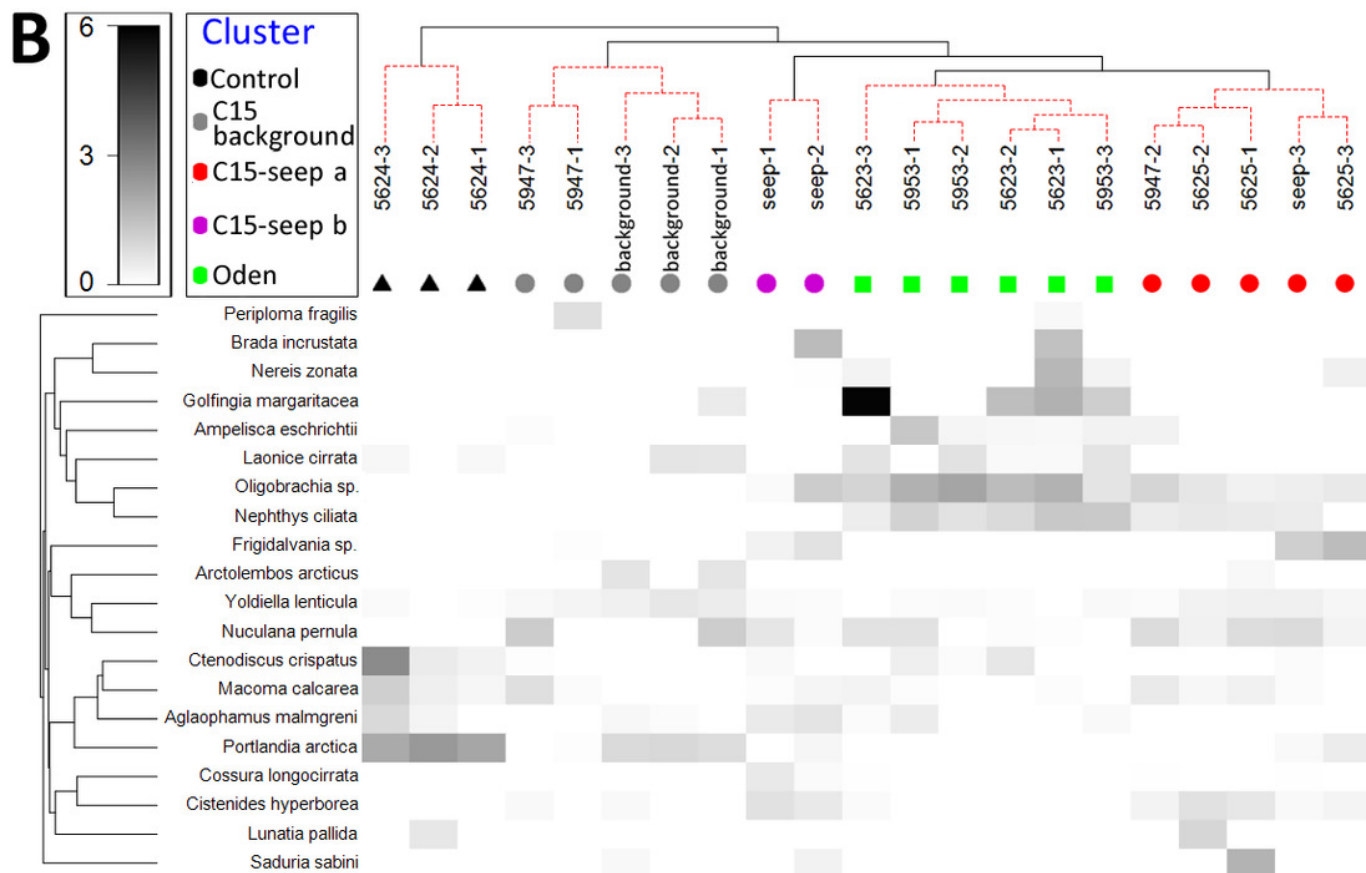
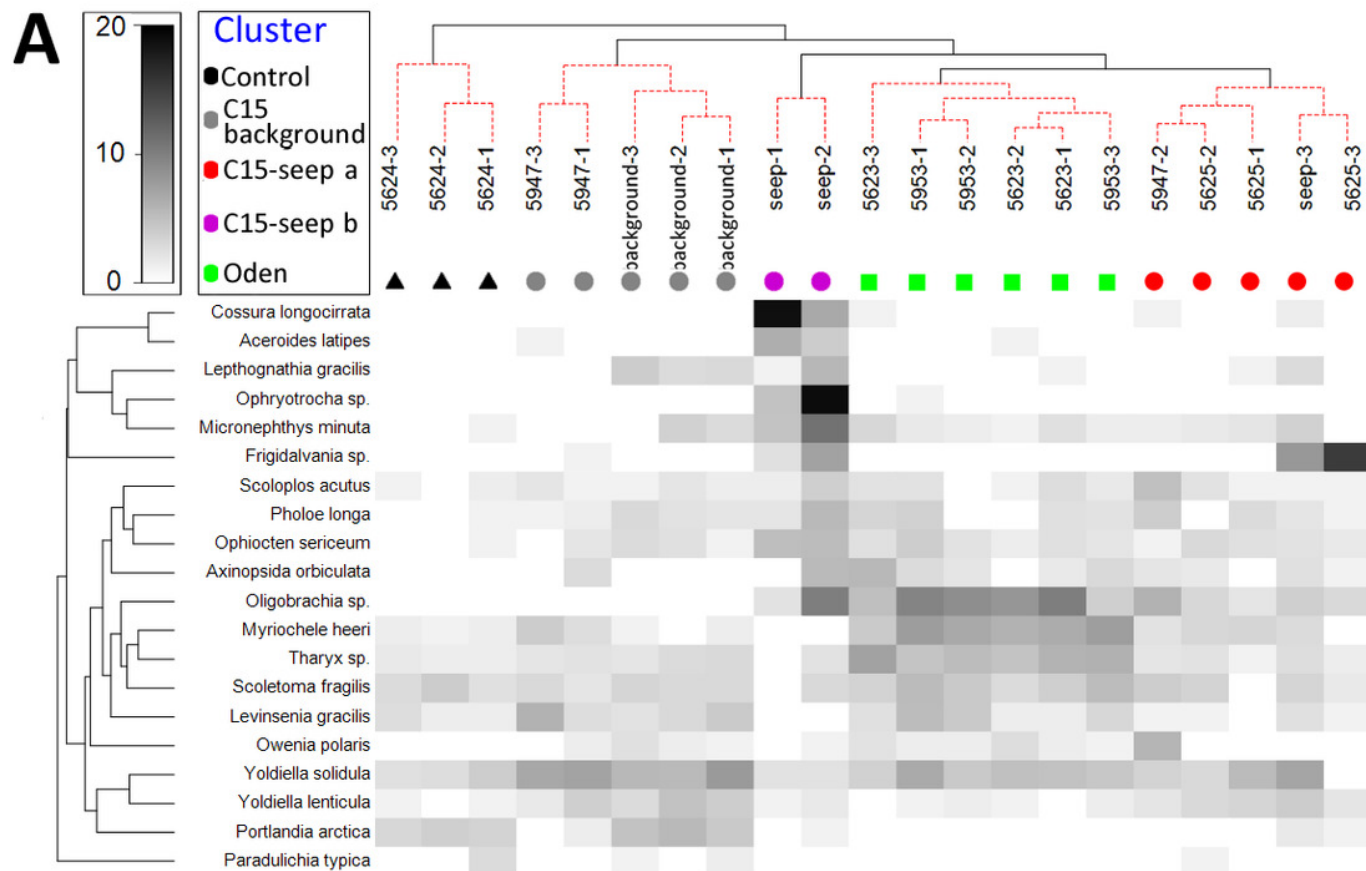


Figure 6

Species ranking for C15 and Oden trawl samples.

The most numerous species are indicated. X-axis is logarithmic.

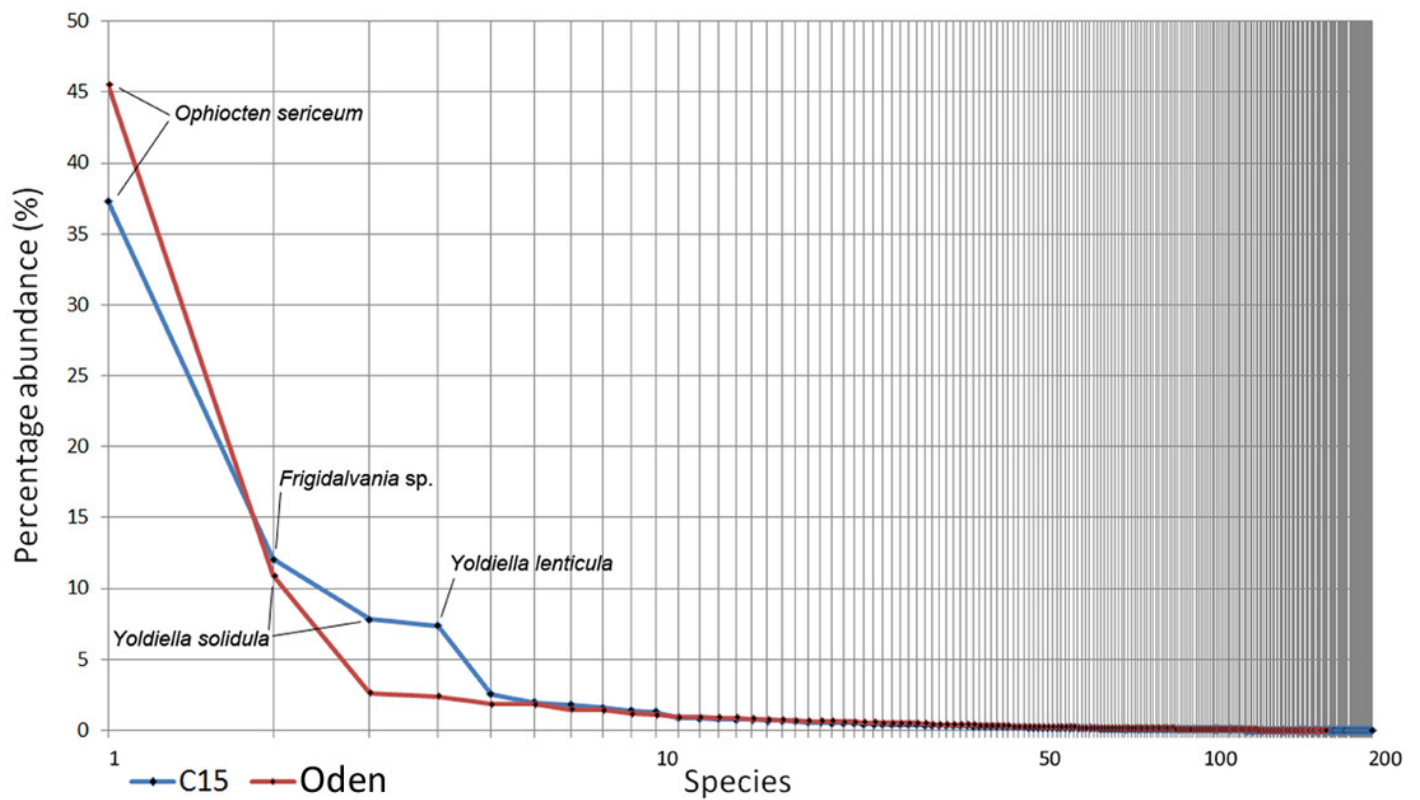


Figure 7

Taxa found only at seep stations.

A - *Oligobrachia* sp. (left - tube with several fragments enlarged; center - complete specimen extracted from tube; right - anterior and posterior fragments of the specimen); B - *Frigidalvania* sp.; C - *Ophryotrocha* sp. (upper left - several specimens, total view; upper right - anterior fragment; lower - enlarged parapodia); D - *Axinopsida orbiculata*. Photos by A. Vedenin and V. Kokarev.

